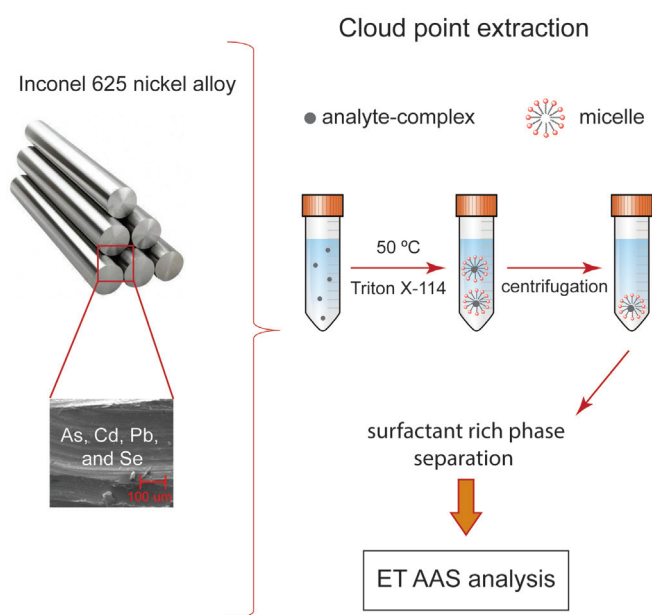


ARTICLE

Systematic Study for Determining As, Pb, Cd, and Se in Steel and Nickel Alloy Samples by GF AAS: Circumventing Matrix Interference with Extraction Based on Micellar Separation

Natália Tostes Canevari Viola , Brian Cardoso Ferreira , Lilian Rodrigues Rosa Souza ,
Márcia Andreia Mesquita Silva da Veiga  

Departamento de Química, FFCLRP, Universidade de São Paulo, 14040-901, Ribeirão Preto, SP, Brazil



This study proposes a matrix separation procedure based on micellar-mediated extraction (cloud point extraction - CPE) for determining As, Cd, Pb, and Se (potential contaminants) in nickel alloy and steel samples. Structural characterization and qualitative analysis of Ni alloy were conducted on the nickel alloy using scanning electron microscopy-energy-dispersive X-ray spectroscopy (SEM-EDS). After sample decomposition, ammonium o,o-diethyl dithiophosphate (DDTP) was used to complex the analytes and Triton X-114 as a non-ionic surfactant in CPE for matrix separation and extraction. Methanol acidified with 0.1 mol L⁻¹ HNO₃ was added to the surfactant-rich phase before the analytes determination by graphite furnace atomic absorption spectrometry (GF AAS). Parameters such as pH, complexing agent and surfactant concentrations, acid medium, complexation time, and type of diluent

were evaluated. The obtained results indicated that the ratio DDTP:As was 3:1, DDTP:Cd and DDTP:Pb was 2:1, and DDTP:Se was 1:1. The enrichment factors were 6, 8, 14, and 13, and limits of detection were 1.5, 0.06, 0.31 and 0.27 µg g⁻¹ for As, Cd, Pb, and Se, respectively. The method was applied for As, Cd, Pb, and Se determination in Inconel 625 nickel alloy and standard reference materials (AISI 4340 Steel - SRM[®] 361, AISI 94B17 Steel - SRM[®] 362, Chromium-Vanadium Steel - SRM[®] 363, and Nickel Alloy UNS - SRM[®] 864). Analyte recoveries lay above 88%, and relative standard deviations were lower than 5%. Application of cloud point extraction for matrix separation allowed the determination of low concentrations of As, Cd, Pb, and Se, constituting an environmentally friendly method.

Cite: Viola, N. T. C.; Ferreira, B. C.; Souza, L. R. R.; da Veiga, M. A. M. S. Systematic Study for Determining As, Pb, Cd, and Se in Steel and Nickel Alloy Samples by GF AAS: *Circumventing Matrix Interference with Extraction Based on Micellar Separation*. *Braz. J. Anal. Chem.* 2024, 11 (42), pp 94-111. <http://dx.doi.org/10.30744/brjac.2179-3425.AR-38-2023>

Submitted 06 April 2023, Resubmitted 06 July 2023, Accepted 09 July 2023, Available 17 online July 2023.

Keywords: steel; nickel alloy; cloud point extraction; As, Cd, Pb, and Se; GF AAS

INTRODUCTION

The production and global trade of metals and alloys are critical to modern industrial infrastructure. Continuous improvement of metallurgical processes and manufacturing technologies have paved the way for developing nickel alloys,¹ commonly employed under circumstances requiring strength and corrosion resistance at high temperatures, e.g., for application in nuclear, chemical, and petrochemical plants as aerospace and navigation industry.² Several factors influence the properties of nickel alloys, including the major constituent elements, the production process, and the thermal treatment of the intermediate product.³ Moreover, the presence of trace contaminants such as Ag, As, Bi, Cd, Pb, Sb, Se, Sn, Te, Tl, and Zn at concentrations above a certain limit may impact the mechanical and magnetic properties of these materials negatively. Remarkably, As, Cd, Pb, and Se can affect the properties related to the mechanical and thermal resistance of steel and nickel alloys by lowering the melting point, which leads to severe disruption and a disastrous failure of the final product.⁴⁻⁶

Quality control with respect to elements concentration is crucial to ensure the development and application of nickel alloys. However, trace elements determination is a challenging task, considering that the alloy matrix is quite complex.⁴ To prevent interferences, matrix separation has been employed in trace element determination.⁷ Cloud point extraction (CPE) has also been employed for purpose; it complies with green chemistry principles⁸ has some advantages: it is safe to operate (the reagents are not volatile or toxic); it generates a lower amount of laboratory residues (small volumes of reagents are used); and it allows pre-concentration of many species with good enrichment factors.^{9,10}

CPE is based on micelles formation by surfactants in aqueous solutions. They promote phase separation upon a change in temperature or the addition of a salting-out agent. The surfactants, above the critical micelle concentration (CMC), can self-assemble in water into supra-molecular aggregates and, when heated at a given temperature (cloud point), result in a biphasic system with a surfactant-rich phase of a small volume containing the hydrophobic compounds initially present in the solution and a surfactant-poor phase that can be separated from the surfactant rich phase. Inorganic species, which are hydrophilic, are extracted in the surfactant-rich phase by using a complexing agent that produces hydrophobic compounds under suitable conditions.^{11,12} Different complexing agents have been used in CPE, e.g., ammonium pyrrolidine dithiocarbamate (APDC),¹³ 1,2-thiazolylazo-2-naphthol (TAN),¹⁴ 8-hydroxyquinoline (8-HQ),¹⁵ and ammonium O,O-diethyl dithiophosphate (DDTP). DDTP has a sulfur atom as the electron donor. They behave like a soft base and can complex elements that are mildly acidic and does not form a stable complex with alkaline metals. This selectivity is desirable since it avoids the potential matrix effects as in the case of metal alloys analysis.^{16,17}

Ammonium O,O-diethyl dithiophosphate has been employed for As preconcentration and subsequent determination in corn and rice samples by hydride generation coupled to atomic fluorescence spectrometry,¹⁸ Cd and Pb in urine¹⁹ and Cd, Pb, and Pd in blood, with subsequent determination using graphite furnace atomic absorption spectrometry (GF AAS).²⁰ DDTP has also been used for As, Bi, Cd, and Pb preconcentration in river water, wine, fertilizer, and urine prior the analytes determination by inductively coupled plasma optical emission spectrometry (ICP OES).²¹

Cloud point extraction has already been employed in the analysis of alloy samples as reported by Kassem and Amin, who determined rhodium in a metallic alloy using 5-(4'-nitro-2',6'-dichlorophenylazo)-6-hydroxypyrimidine-2,4-dione (NDPHPD) as a complexing agent and Triton X-114 as a surfactant²² and Bahchevanska et al. determined vanadium in aluminum alloy using 1-(2-thiazolylazo)-2-naphthol (TAN) and complexing agent and Triton X-114 as a surfactant.²³ However, this approach has yet to be explored for other elements and metal alloys.

In the present work, CPE is proposed for As, Cd, Pb and Se separation from Ni alloy and steel digestates of cloud point extraction, followed by the determination of analytes by GF AAS. The proposed CPE procedure involves analyte extraction with the complexing agent DDTP in the presence of the non-ionic surfactant Triton X-114.

MATERIALS AND METHODS

Samples

Carbon steel saw was employed to cut the nickel alloy sample (Inconel 625) into the most diminutive possible dimensions. After this procedure, pieces with a rectangular shape, measuring 1x1 cm and weighing approximately 2.5 g, were obtained. For accuracy evaluation, samples of the following standard reference materials (CRMs) were analysed: AISI 4340 Steel (SRM[®] 361), AISI 94B17 Steel (SRM[®] 362), Chromium-Vanadium Steel (SRM[®] 363), and Nickel Alloy UNS N06600 (SRM[®] 864), produced at the National Institute of Standards and Technology (NIST).

Reagents and solutions

Experiments were performed with reagents of analytical grade. Ultrapure water (resistivity of 18.2 MΩ cm⁻¹), obtained from a Milli-Q[®] water purification system (Millipore, Billerica, MA, USA), was used to prepare the reagents and solutions. All the glassware was decontaminated in 30% (v v⁻¹) HNO₃ for 48 h and rinsed in ultrapure water for a few minutes.

To decompose the Inconel 625 nickel alloy sample and CRMs, 37% m m⁻¹ HCl (JT Baker) and 65% m m⁻¹ HNO₃ (JT Baker) were employed.

Concerning CPE, the Cd and Pb solutions were prepared by diluting stock standard solutions containing 1000 mg L⁻¹ of the respective analytes (Titrisol[®] standards from Merck). A standard stock solution of 4000 mg L⁻¹ As was prepared by dissolving 0.1 g of As₂O₃ (Acros) in 25 mL of previously heated water containing 3 mL of 37% m m⁻¹ HCl (JT Baker). A 7.5 mg L⁻¹ Se(IV) solution was obtained from a 1000 mg L⁻¹ standard solution of Se(VI) (Fluka) by heating this solution in 6 mol L⁻¹ HCl for 30 min at 100 °C. A 5% (m v⁻¹) ammonium o,o-diethyl dithiophosphate solution was prepared daily using the DDTP ammonium salt (Aldrich) dissolved in deionized water. 37% m m⁻¹ HCl (JT Baker) was employed to adjust pH of solutions. A 5% (m v⁻¹) octylphenoxypolyethoxyethanol (Triton X-114) solution was prepared by weighing 2.5 g of the reagent (Sigma-Aldrich) in a graduated tube followed by the addition of 50 mL of water. To reduce the viscosity of the surfactant-rich phase, methanol (Panreac) acidified with 0.1 mol L⁻¹ HNO₃ was used. Ascorbic acid (Sigma-Aldrich) and citric acid (Carlo Erba) were used for Fe and Ni interference studies, respectively. The chemical modifier Pd(NO₃)₂ + Mg(NO₃)₂ employed in Cd and Pb determination was prepared by mixing 1 mL of Pd(NO₃)₂ 10 g L⁻¹ (Fluka) and 100 μL of Mg(NO₃)₂ 10 g L⁻¹ (Merck) in a graduated flask, followed by addition of 10 mL of deionized water. For As, Pd(NO₃)₂ was employed as chemical modifier, which was prepared by diluting 1 mL of 10 g L⁻¹ Mg(NO₃)₂ in 10 mL of water in a graduated flask. For Se, Ni + Mg(NO₃)₂ was used as chemical modifier, which was prepared by mixing 801 μL of 1000 mg L⁻¹ Ni standard solution (Fluka) and 79 μL of 10 g L⁻¹ Mg(NO₃)₂, followed by the addition of 1 mL of water.

Instrumentation

The nickel alloy sample and CRMs were decomposed in a metallic block (TE-040/25, Tecnal, Piracicaba, São Paulo, Brazil). For the CPE experiments, a water bath with controlled temperature (MA127, Marconi, Piracicaba, São Paulo, Brazil) and a centrifuge (Z 326K, Hermle Labortechnik, Wehingen, Germany) were employed.

Arsenic, Cd and Se were determined using an atomic absorption spectrometer (AAAnalyst 800, PerkinElmer, Norwalk, CT, USA) whereas Pb was by using with a high-resolution continuum source atomic absorption spectrometer (ContraAA 700, Analytik Jena AG, Jena, Germany). Both instruments were equipped with an autosampler for sample introduction and a transversely heated pyrolytic graphite tube. Twenty microliters of sample or reference solutions, 5 μL of the chemical modifiers Pd(NO₃)₂ + Mg(NO₃)₂ for Cd and Pb and Pd(NO₃)₂ for As, or 10 μL of Ni + Mg(NO₃)₂ for Se were pipetted into the graphite tube. Argon with 99.998% purity (White Martins, Sertãozinho, São Paulo, Brazil) was used as the purge gas. Tables SI and SII (Supplementary information) summarize the instrumental parameters.

The graphite furnace temperature programs given in Tables SIII and SIV were run during As, Cd, Se, and Pb determination.

Structural characterization of the nickel alloy sample

The structural characterization and qualitative analysis of the Inconel 625 nickel alloy sample were carried out using a scanning electron microscope (EVO 50, ZEISS - Carl Zeiss, Cambridge, England) equipped with an EDS system (IXRF Systems 500 Digital Processing Si(Li) diode, Liechtenstein). The detector was employed in the secondary electron mode, the chamber pressure was 1.8×10^{-5} Torr, and the accelerating voltage was 20 kV.

To avoid possible contamination during the cut of the Inconel 625 sample. It was placed in a glass beaker containing 50 mL of 2-propanone (Merck) and sonicated in an ultrasonic bath (USC-1400, Unique, Indaiatuba, São Paulo, Brazil) for 15 min.

Sample preparation

Regarding the decomposition of the nickel alloy sample before As, Cd, and Se determination, each fragment was weighed (2.5 g of a fragment of 1x1 cm), placed in a glass flask, to which with 24 mL of an acid mixture containing 37% HCl (m m^{-1}) and 65% HNO_3 (m m^{-1}) (3:1 ratio) were added. Experiments were conducted in triplicate. The flasks were placed in a digester block, and the mixture was heated from 50 to 85 °C. Between 2 and 4 h was required for complete sample digestion. After cooling, the solutions were transferred to graduated tubes, and the volume was adjusted to 30 mL with water. This procedure was also applied to check the analytes recovery, where sample aliquots were spiked to obtain $20 \mu\text{g L}^{-1}$ As, $0.45 \mu\text{g L}^{-1}$ Cd, $10 \mu\text{g L}^{-1}$ Pb, and $8 \mu\text{g L}^{-1}$ Se to assay analyte recoveries. The sample solutions were then submitted to CPE. The same methodology was employed to decompose the standard reference materials; however, in this case, the sample mass was 0.250 g, and the volume of the acid mixture was 8 mL.

For Pb, 25 mL of 65% (m m^{-1}) HNO_3 were added to the sample. The mixture was heated at 50 to 120 °C for 24 h in this case, a more extended period was necessary for complete sample decomposition. Analyte recovery was assessed for samples aliquots spiked to contain $10 \mu\text{g L}^{-1}$ Pb. The same procedure was followed to decompose the CRMs; however, the sample mass was 0.250 g, and the 65% HNO_3 (m m^{-1}) volume was 5 mL.

Cloud point extraction

Initially, aliquots of digestate (100 μL), ascorbic acid (0.1 g) (for the elimination of Fe interference), and 37% HCl (m m^{-1}) (for pH adjustment, ensuring the best absorbance for each analyte) were transferred to graduated flask. The volume was adjusted to 9 mL with water, and the mixture left to rest during 15 min for the complete dissolution of the ascorbic acid. Subsequently, different amounts of DDTP solution were added (according to the optimization of CPE parameters) and the solution left resting for 20 min. Then, Triton X-114 was added, and the volume was adjusted to 15 mL with water. The solutions were heated in a water bath at 50 °C for 20 min, followed by centrifugation at 1233 G for 20 min. Next, the flasks were immersed in an ice bath for 15 min and then the supernatant aqueous phase was removed with a micropipette. 500 μL of methanol containing 0.1 mol L^{-1} HNO_3 was added to the extracts to reduce the viscosity of the surfactant-rich phase before the determination of analytes by GF AAS. Calibration solutions and analytical blanks were also submitted to CPE in the same conditions as the samples. The concentrations of DDTP, Triton X-114, and HCl, the acid medium for complexation, the type of diluent for the surfactant-rich phase, and the complexation time were evaluated.

Optimization of CPE

Analyte preconcentration using CPE requires careful optimization of experimental parameters because it affects the extraction efficiency, phases separation and enrichment factor. As such the HCl, complexant, and surfactant concentrations, acid medium, complexation time, and type of diluent of the surfactant-rich phase were considered.

The complexation time was for 20 min, and 0.1 mol L^{-1} HNO_3 in methanol was used to dilute the surfactant-rich phase unless stated otherwise.

RESULTS AND DISCUSSION

Structural characterization of the nickel alloy sample

The structural characterization and qualitative analysis were carried out using scanning electron microscopy-energy-dispersive X-ray spectroscopy (SEM-EDS). In Figures 1 and 2 shows the SEM-EDS images obtained from the nickel alloy sample.

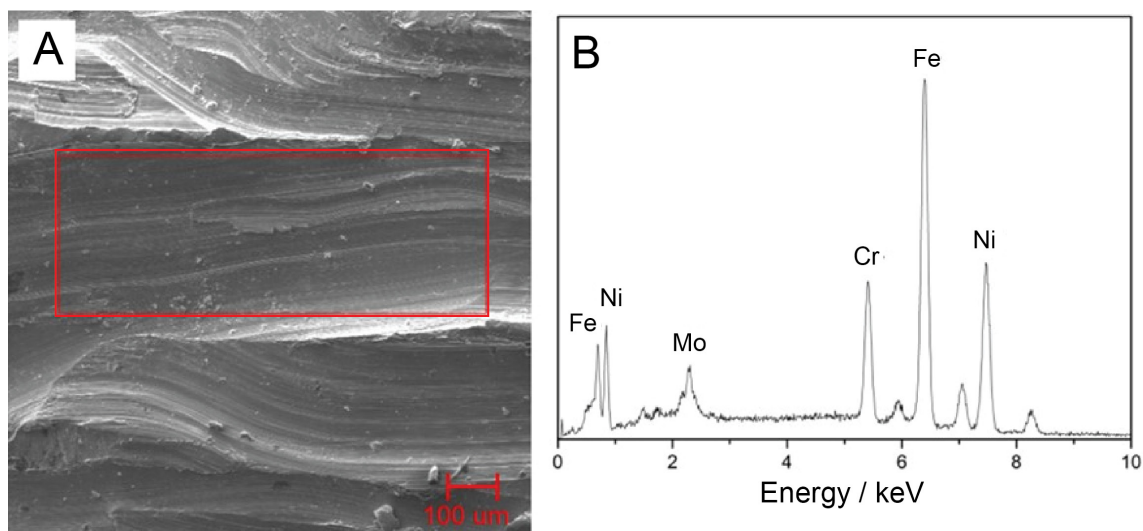


Figure 1. Image obtained of the nickel alloy sample by SEM-EDS in the secondary electron mode (a) and respective EDS spectrum (b).

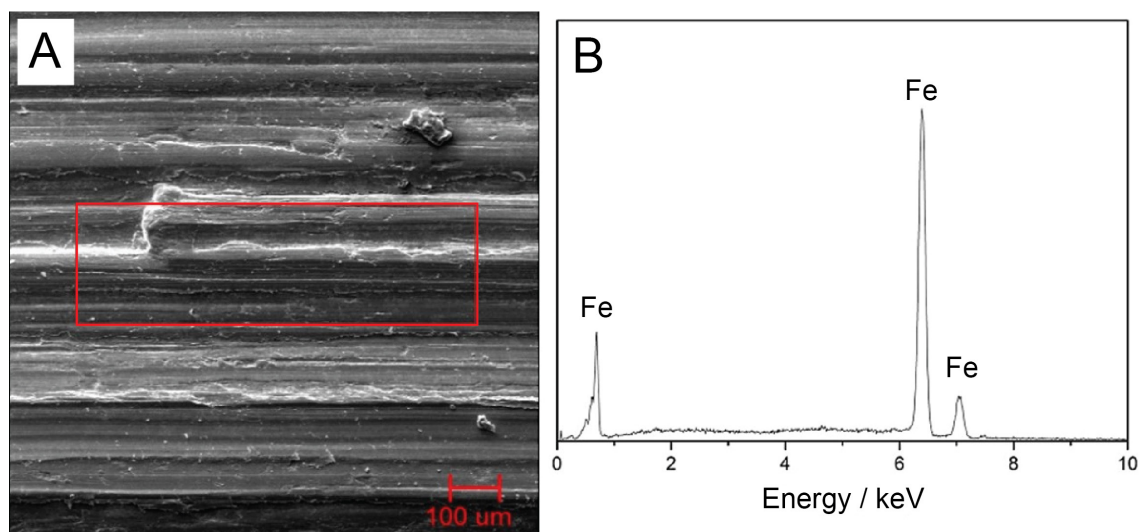


Figure 2. Image obtained of the internal structure of the nickel alloy sample by SEM-EDS (a) and respective EDS spectrum (b).

All the SEM imaging was carried out using the secondary electron mode, which can provide helpful information about the material surface and topography. Considering the analyzed region, represented in red color in Figure 1 (a), the surface portion of the nickel alloy sample demonstrates that Cr, Fe, and Ni were present in this material, constituting respectively, 11, 44 and 33% of the analyzed portion. Besides, Nb (2%) and Mo (4%) were also present in this portion. The presence of these elements was expected, as they are constituents of the Inconel 625 nickel alloy.^{24,25}

With respect to the images of Ni internal portion, Figure 2 (a) and (b), elements present were Fe (94%) oxygen (5%), and carbon (1%). Unlike the surface portion, Ni and Cr were not observed. This is due to the differences of the material, as the surface has a coating of Inconel 625, and the internal part is carbon steel.

Identifying the major chemical elements is possible using SEM-EDS; however, the elements evaluated in this study (As, Cd, Pb, and Se) were not detected. The SEM-EDS technique does not have sufficient sensitivity to detect elements present as impurities in the alloy, reinforcing the need to employ other techniques to ensure the quality control of the alloy. These elements (as impurities) are commonly present in Ni alloys in concentration below 100 mg kg^{-1} and therefore, not detected using SEM-EDS.

Concentration of DDTP

The complexing agent concentration must be enough to compensate for any reagent consumption by other elements that can compete with the analytes. Furthermore, complexing agents with lower partition coefficients must be present in large excess for efficient analytes complexation and subsequent separation.²⁶

In this study, the DDTP concentrations evaluated, ranged from 0 to 2% (m v^{-1}) for As and Pb, 0 to 3% (m v^{-1}) for Cd, and from 0 to 0.3% (m v^{-1}) for Se. Figure 3 shows how the As, Cd, Pb, and Se absorbances changed as a function of the logarithm of the DDTP concentration. The As signal increased with the DDTP concentration increase up to 0.5% (m v^{-1}) of DDTP. After that, the As signal decreased gradually because charged complexes were produced at higher DDTP concentrations. This phenomenon can reduce the extraction efficiency because uncharged complexes are preferentially extracted in the hydrophobic core of the micelles.^{16,26} Furthermore, according to Fiorentini et al., the excess of DDTP reduces the As absorbance, which can be attributed to the increase in the organic content injected in the atomizer.²⁷ For 0.5% (m v^{-1}) DDTP the highest absorbance of As was observed.

The Cd absorbance increased up to 1% (m v^{-1}) of DDTP. It stabilized around 0.3% (m v^{-1}) of DDTP, increased slightly up to 1% (m v^{-1}) of DDTP, and then decreased. The Pb absorbance also increased with the DDTP concentration increase up to 1% (m v^{-1}) DDTP. Regarding to Se, its absorbance was slightly affected by the DDTP concentration whereas the highest absorbance was observed for 0.06% (m v^{-1}) DDTP. Thus, considering the highest absorbance observed, the DDTP concentration in the later experiments was 0.5% (m v^{-1}) for As, 1% (m v^{-1}) for Cd and Pb, and 0.06% for Se.

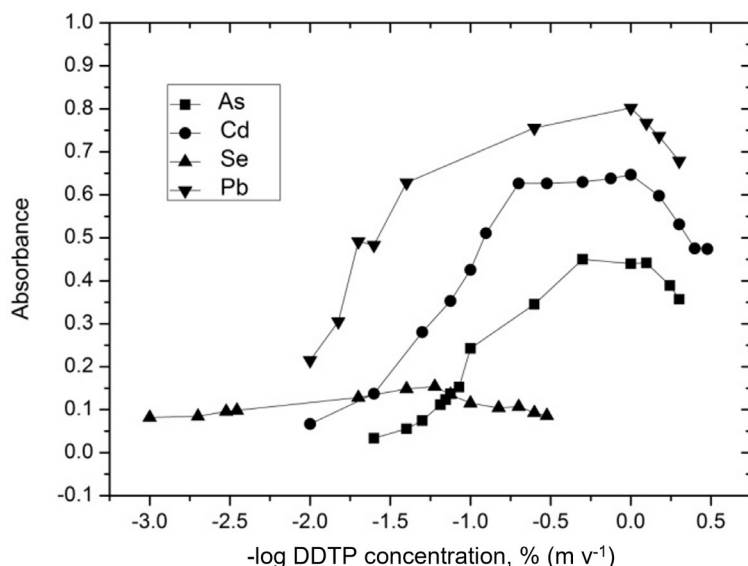


Figure 3. Effect of DDTP concentration on $50 \mu\text{g L}^{-1}$ As(III), $1 \mu\text{g L}^{-1}$ Cd(II), $20 \mu\text{g L}^{-1}$ Pb(II), and $10 \mu\text{g L}^{-1}$ Se(IV) in the following conditions: As - 0.96 mol L^{-1} HCl, 0.5% (m v^{-1}) Triton X-114; Cd - 0.3 mol L^{-1} HCl, 1% (m v^{-1}) Triton X-114; Pb - 0.32 mol L^{-1} HCl, 1% (m v^{-1}) Triton X-114; Se - 0.1 mol L^{-1} HCl, 0.2% (m v^{-1}) Triton X-114. ($n = 3$).

The differences observed in Figure 3 are due to the affinity of the elements with the DDTP affinities, according to Pearson's theory, which will be discussed further in section "Determination of the ratio DDTP: analysis in the complex".

Concentration of HCl

Optimizing the pH is also crucial for CPE, especially for ionizable species such as metals. An appropriate pH range is mandatory in which uncharged analyte species exist and can be incorporated into micelles, allowing a quantitative extraction of the analyte.²⁸

The cloud point increases with the solution pH decrease because the attractive forces between the surfactants and the water molecules increase. Consequently, surfactant molecules become more repulsive, leading to lower extraction efficiency and a smaller volume of the surfactant-rich phase. In addition, high acid concentration and temperature can accelerate DDTP decomposition,²⁹ mainly if HNO_3 is used, as it is a strong oxidant.

In the present study HCl concentrations ranging from 0 to 1 mol L⁻¹ HCl for As, Cd, and Se and from 0 to 0.75 mol L⁻¹ HCl for Pb were evaluated to find the best conditions for CPE. Figure 4 illustrates how the HCl concentration affected the As, Cd, Pb, and Se absorbances. The As absorbance increased when the HCl concentration was up 0.32 mol L⁻¹ HCl, but remained constant for HCl concentrations above 0.32 mol L⁻¹ (pH = 0.49). The Cd absorbance remained constant for 0.1 to 0.2 mol L⁻¹ HCl, increased slightly for 0.32 mol L⁻¹ HCl and stabilized afterward. Hence, 0.32 mol L⁻¹ HCl was used in subsequent experiments for Cd and As. The more appropriate HCl concentration for the Pb CPE was 0.1 mol L⁻¹ (pH = 1), considering that it corresponded to the highest absorbance for of Pb. The maximum Se absorbance was observed using 0.1 mol L⁻¹ HCl. Therefore, 0.1 mol L⁻¹ HCl was used for Cd and Ob in further experiments.

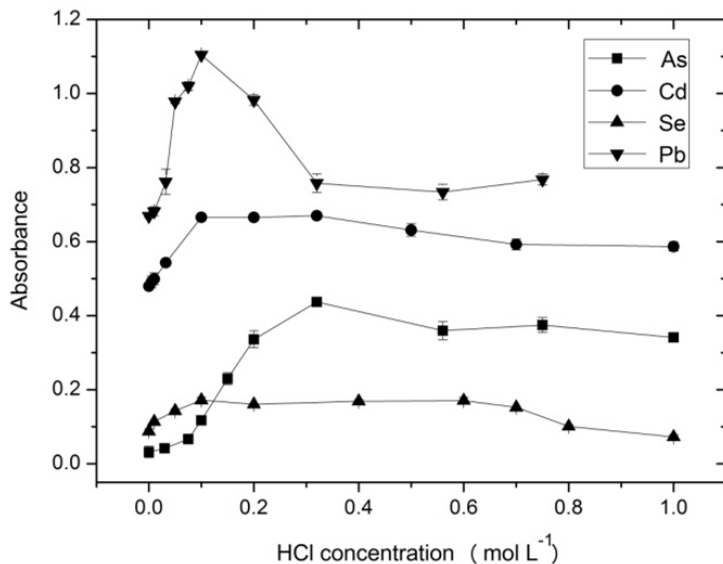


Figure 4. Effect of HCl concentration on 50 $\mu\text{g L}^{-1}$ As(III), 1 $\mu\text{g L}^{-1}$ Cd(II), 20 $\mu\text{g L}^{-1}$ Pb(II), and 10 $\mu\text{g L}^{-1}$ Se(IV) in the following conditions: As - 0.5% (m v⁻¹) DDTP, 0.5% (m v⁻¹) Triton X-114; Cd and Pb - 1% (m v⁻¹) DDTP, 1% (m v⁻¹) Triton X-114; Se - 0.06% (m v⁻¹) DDTP; 0.2% (m v⁻¹) Triton X-114. (n = 3).

Triton X-114 concentration

An effective CPE also depends on the surfactant concentration. The surfactants molecules can aggregate above the CMC and form micelles where the complexed analyte is retained. The analyte extraction from solution increases with the increasing surfactant concentration up to a maximum value,

providing quantitative analyte recovery. If the surfactant concentration is too high both the extraction and preconcentration factor are worsened; excess of surfactant increases the volume of the surfactant rich phase that became too diluted.³⁰

On the other hand, if the surfactant concentration is lower than the necessary it results in inefficient extraction analyte, probably because the micelles cannot capture the hydrophobic complexes quantitatively.²⁰ In this study, the surfactant Triton X-114 was employed because it has a relatively low CPE temperature (between 22 and 25 °C), is low cost and is not volatile or toxic.⁹

The Triton X-114 concentration influence on the analytes absorbances is depicted in Figure 5. Triton X-114 at 1% ($m v^{-1}$) yield the highest As absorbance As, and this concentration was selected for As. For Triton X-114 concentrations below 0.05% ($m v^{-1}$), a surfactant-rich phase was not obtained; i.e., the critical micelle concentration (CMC) and/or cloud point were not attained under the experiment conditions. Concerning Cd, the volume of the surfactant-rich phase obtained at higher Triton X-114 concentrations was visible. The absorbance increased until the surfactant concentration was 0.5% ($m v^{-1}$) decreasing thereafter, and the same condition was observed for Pb. Therefore, 0.5% ($m v^{-1}$) Triton X-114 was further employed for Cd and Pb experiments. The same concentration of Triton X-114 (0.6%) was also used in the determination of Cd in food, by to Anzum et al.³¹ On the other hand, Rihana-Abdallah employed a lower Triton X-114 concentration (0.2%) in Pb and Cd determination in water samples using CPE.³² Regarding to Se, the highest absorbance was observed when the Triton X-114 concentration was 0.1% ($m v^{-1}$). For surfactant concentrations lower than 0.025% ($m v^{-1}$) solution turbidity and phase separation were not observed. As such, 0.1% ($m v^{-1}$) Triton X-114 was adopted for Se.

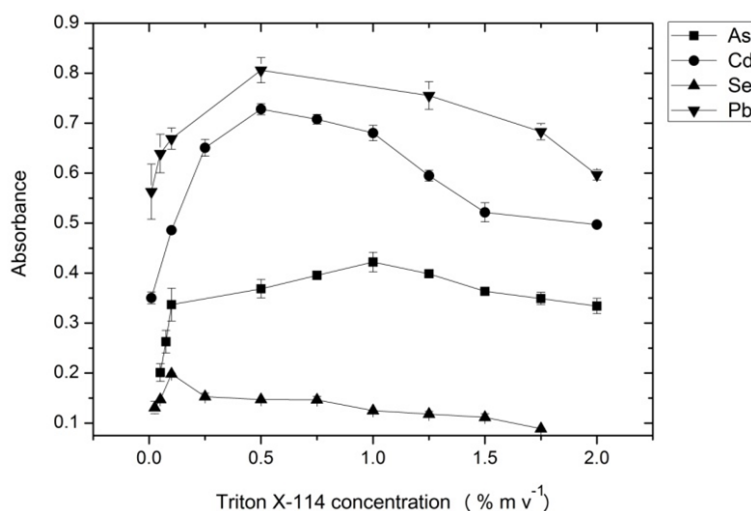


Figure 5. Effect of Triton X-114 concentration on $50 \mu g L^{-1} As^{3+}$, $1 \mu g L^{-1} Cd^{2+}$, $20 \mu g L^{-1} Pb^{2+}$ and $10 \mu g L^{-1} Se^{4+}$ in the following conditions: As - 0.5% ($m v^{-1}$) DDTP, 0.32 mol L^{-1} HCl; Cd - 1% ($m v^{-1}$) DDTP, 0.32 mol L^{-1} HCl; Pb - 1% ($m v^{-1}$) DDTP, 0.1 mol L^{-1} HCl; Se - 0.06% ($m v^{-1}$) DDTP, 0.1 mol L^{-1} HCl.

Considering the stability of DDTP in strong acid medium,¹⁶ a study was conducted to determine the appropriate medium for the analyte complexation and subsequent CPE; 0.96 mol L^{-1} HCl or HNO_3 (pH = 0.018), 0.3 mol L^{-1} HCl or HNO_3 (pH = 0.5) and 0.32 mol L^{-1} HCl or HNO_3 (pH = 0.49) were used for As, Cd, and Pb, respectively. It was observed that the absorbances of the analytes were not affected by the type and acid concentration. However, considering the oxidant property of HNO_3 , which can react with the DDTP and degrade it,³³ HCl (0.1 mol L^{-1} for Pb and Se, and 0.32 mol L^{-1} for As and Cd) was the acid adopted for CPE of As, Cd and Pb. For Se, the effect of HCl concentration was not evaluated, since Se (VI) must be reduced to Se (IV) because DDTP complex only with Se (IV). To this end, before the CPE

procedure the Se(VI) solution in 6 mol L⁻¹ HCl was heated at 100 °C³⁴ for 30 min. This step is crucial to guarantee that all Se is present as Se(IV) since only this Se species complexes with DDTP.¹⁷

To verify whether the type of diluent for the surfactant-rich phase could influence the analyte signal, methanol, ethanol, and methanol or ethanol acidified with 0.1 mol L⁻¹ HNO₃ were evaluated. Differences for As, Cd, Pb, and Se absorbances were not observed for the diluents evaluated. However, considering that methanol is volatile and adding HNO₃ favors its stabilization via hydrogen bonding, methanol with 0.1 mol L⁻¹ HNO₃ was chosen as diluent of the surfactant-rich phase for the four analytes.

The complex formation rate is worth considering in the case of species separation by CPE. Complexation time is a critical parameter for on-line procedures as it requires the reaction to be as complete as possible in a short time for efficient extraction. The complexation time between the analytes and DDTP was evaluated and there were no significant differences for time periods up to 60 min. Hence, the previously adopted time of 20 min was maintained. The optimized conditions of CPE are summarized in Table I.

Table I. Optimized conditions for CPE

Parameter	As	Cd	Pb	Se
DDTP (% m v ⁻¹)	0.5	1	1	0.06
HCl (mol L ⁻¹)	0.32	0.32	0.1	0.1
Triton X-114 (% m v ⁻¹)	1	0.5	0.5	0.1
Time (min)	20	20	20	20
Diluent	Methanol in HNO ₃			

Determination of the ratio DDTP: analysis in the complex

Da Silva et al.²⁹ have developed a mathematical approach based on the absorbance values in the graph constructed for the optimized DDTP concentration, to determine the ratio between the ligand and the analyte in the complex formed in a study dealing with CPE.

The distribution ratio (D) is the ratio between the complex analyte concentration in the surfactant-rich phase and the analyte concentration in the aqueous phase. This parameter is essential for CPE because the more hydrophobic the surfactant, the greater the D value. In this study, D values were calculated from normalized absorbance values obtained from the DDTP concentration optimization graph for As, Cd, Pb, and Se (Figure 3), according to Equation 1:

$$D = \frac{(A_c - A_0)}{(A_\infty - A_c)} \quad \text{Equation 1}$$

A_c is the analyte absorbance for a given DDTP concentration, A₀ is the absorbance when no ligand is used, and A_∞ is the absorbance for the maximum extraction. Under the conditions used in this study, the free ligand concentration was assumed to be approximately equal to the total ligand concentration.

Values of D calculated with Equation 1 were employed to obtain Equation 2, where n is the charge of the analyte ion in the complex, K_p' , β_n' , and [HL] are the conditional distribution constant, total formation constant, and the free ligand concentration, respectively.

$$\log D = \log (K_p' \beta_n') + n \log [HL] \quad \text{Equation 2}$$

Considering that the pH is constant, the charge (n) of the analyte ion in the complex can be found using Equation 3.

$$n = \left(\frac{\partial \log D}{\partial \log [HL]} \right)_{pH} \quad \text{Equation 3}$$

The value of n also can be found by plotting of the logarithm of D ($\log D$) versus the logarithm of free ligand concentration ($\log [DDTP]$) for As, Cd, Pb, and Se gives straight lines, and the angular coefficient provides information on the ligand/analyte proportion in the complex formed (which is the value of n), according to Figure 6. The absorbance values taken from linear regions of the graphs shown in Figure 3; 0 to 0.1, 0 to 0.125, 0 to 0.04 and 0 to 0.0035% ($m v^{-1}$) for As, Cd, Pb, and Se, respectively.

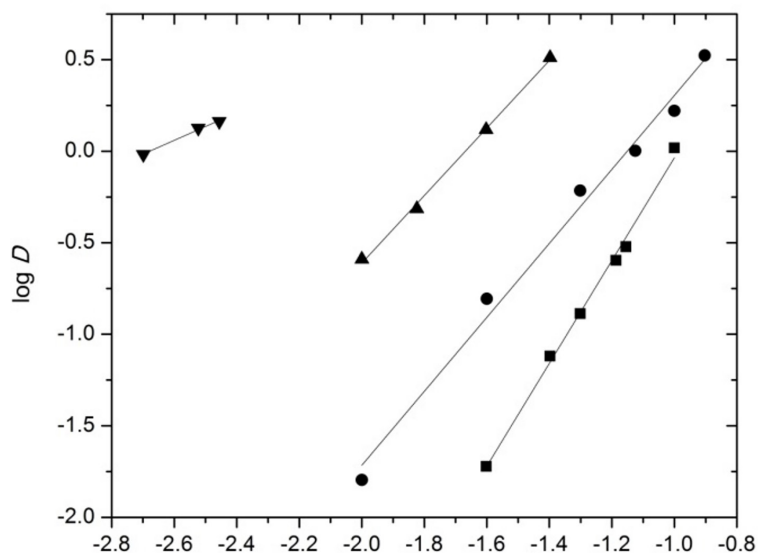


Figure 6. Determination of the proportion between DDTP and As (■), Cd (●), Pb (▲), and Se (▼).

For As, the angular coefficient of the line shown in Figure 6 was 2.81, which indicates a 3:1 ratio DDTP:analyte. This ratio value had not yet been reported for As complexed with DDTP. The logarithm of the product of conditional constants K_p (distribution constant) and β_n (total formation constant) ($\log K_p' \beta_n'$) obtained from equation 2 was 2.77.

The angular coefficient values of the lines (Figure 6) for Cd and Pb were 2.02 and 1.84, respectively, corresponding to a 2:1 ratio DDTP:analyte. This is consistent with the value reported by Borges et al.²⁰ The logarithm values of the product of conditional constants ($\log K_p' \beta_n'$) for Cd and Pb were 2.35 and 3.08, respectively. Regarding Se, the angular coefficient of the line in from the graph of Figure 6 was 0.8, which indicates a 1:1 ratio DDTP:analyte. The pH of the medium was 1.0 where the predominant species of Se are monovalent dimers.³⁵ Moreover, the logarithm of the product of conditional constants ($\log K_p' \beta_n'$) was equal to 2.02.

According to the Pearson acid base concept, DDTP is a soft base and forms complexes preferentially with soft (Cd^{2+}) and borderline acids (Pb^{2+}). Se^{4+} and As^{3+} are defined as hard acids³⁰ and also complex with DDTP, however, as calculated, the conditional constants are lower than for Pb. Considering that the product of the conditional constants ($\log K_p' \beta_n'$) indicates the extent of the reaction between the analytes and DDTP is:

$$2.02 \text{ (Se)} < 2.35 \text{ (Cd)} < 2.77 \text{ (As)} < 3.08 \text{ (Pb)}$$

It demonstrates that the distribution of the species between the aqueous and the surfactant-rich phases is influenced not only by the complexation with DDTP but also by the oxyethylene units in the Triton X-114 molecule.

Pyrolysis and atomization curves

The pyrolysis and atomization temperatures were optimized by constructing pyrolysis and atomization curves for As, Cd, Pb, and Se (Figure 7). Experiments were conducted using reference solutions of the respective analytes and solutions of acid digested Inconel 624 sample to evaluate matrix effect. All solutions were submitted to CPE at the optimized conditions.

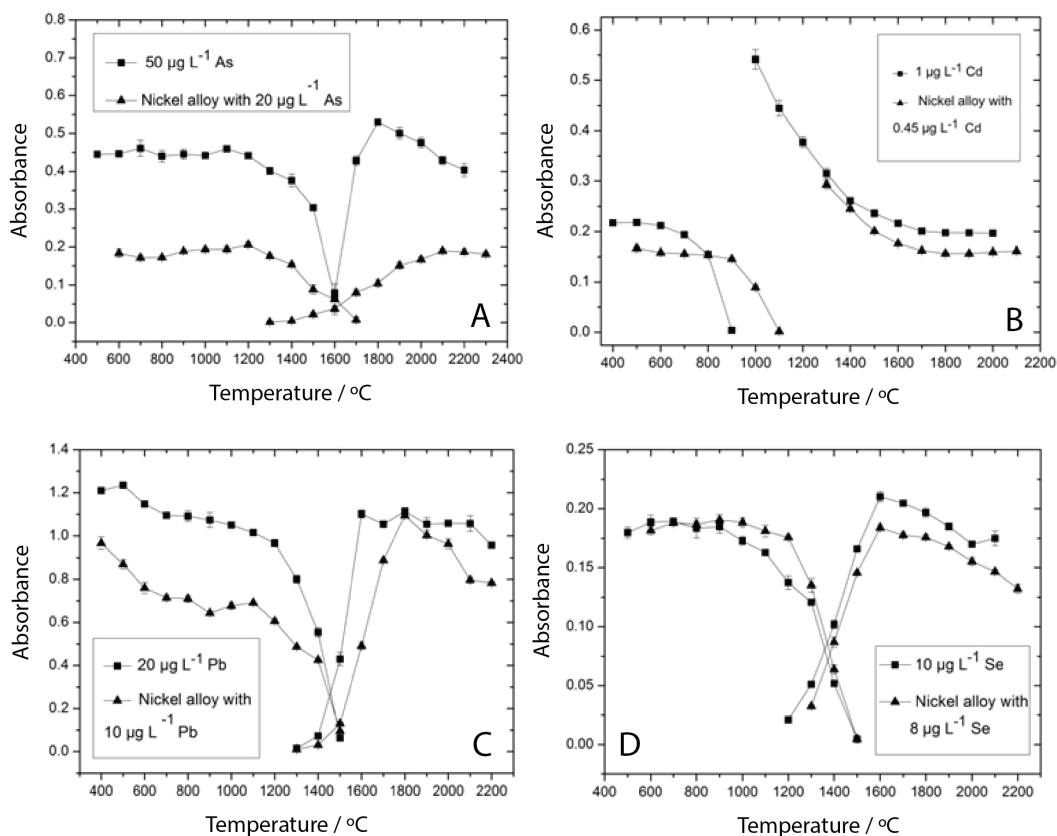


Figure 7. Pyrolysis and atomization temperature curves for (A) 50 $\mu\text{g L}^{-1}$ As and nickel alloy sample solution spiked with 20 $\mu\text{g L}^{-1}$ As. Conditions: 0.5% (m v^{-1}) DDTP, 0.32 mol L^{-1} HCl, 1% (m v^{-1}) Triton X-114; (B) 1 $\mu\text{g L}^{-1}$ Cd and nickel alloy sample spiked with 0.45 $\mu\text{g L}^{-1}$ Cd. Conditions: 1% (m v^{-1}) DDTP, 0.32 mol L^{-1} HCl, 0.5% (m v^{-1}) Triton X-114; (C) 20 $\mu\text{g L}^{-1}$ Pb and nickel alloy sample spiked with 10 $\mu\text{g L}^{-1}$ Pb. Conditions: 1% (m v^{-1}) DDTP, 0.1 mol L^{-1} HCl, 0.5% (m v^{-1}) Triton X-114; and (D) 10 $\mu\text{g L}^{-1}$ Se and nickel alloy sample spiked with 8 $\mu\text{g L}^{-1}$ Se. Conditions: 0.06% (m v^{-1}) DDTP, 0.1 mol L^{-1} HCl, 0.1% (m v^{-1}) Triton X-114. All solutions were submitted to CPE.

Figure 7A depicts the pyrolysis and atomization curves obtained, in both solutions the element absorbance was almost stable up to 1200 °C and then decreased. Therefore, this pyrolysis temperature was adopted in As determination in the samples. Regarding the atomization temperature, more symmetrical and stable peak arose at 2000 °C for As in reference solution, and although the absorbance increased at temperature higher than 2200 °C for spiked sample, to avoid compromising accuracy, the temperature adopted for As determination in the samples was 2000 °C.

As shown in Figure 7B, the Cd absorbance for reference solution remains almost stable for temperature in the range of 400 to 700 °C while the absorbance for spiked sample solution remains stable up to 900 °C. On the other hand, a similar behavior on the Cd absorbance is observed for both solutions in respect to the atomization temperature. Thus, the pyrolysis and atomization temperatures used for Cd determination in the samples were 700 and 1300 °C, respectively.

The pyrolysis and atomization temperatures curves for Pb in Figure 7C demonstrate similar absorbance behavior for both solutions. The pyrolysis and atomization temperatures chosen for Pb were 900 and 1900 °C. They were chosen in view of the better shape of transient signals observed.

Concerning Se, whose pyrolysis and atomization temperature curves are shown in Figure 7D, similar absorbance is observed for both solutions. Thus, taking into account the highest observed absorbance and signal stability, the pyrolysis and atomization temperatures chosen for Se in the analysis of the samples were 900 and 1600 °C, respectively.

Figures of merit of the method

Table II lists the figures of merit of the developed method for As, Cd, Pb, and Se determination in Ni alloy and parameters of calibration curves.

Table II. Figures of merit and parameters of calibration curves

Analytical parameter	Analyte			
	As	Cd	Pb	Se
Limit of detection ($\mu\text{g L}^{-1}$; $\mu\text{g g}^{-1}$)	0.8; 1.5	0.01; 0.06	0.2; 0.3	0.1; 0.3
Limit of quantification ($\mu\text{g L}^{-1}$; $\mu\text{g g}^{-1}$)	2.8; 5.0	0.04; 0.2	0.6; 1.0	0.5; 0.9
Linear correlation coefficient	0.996	0.998	0.999	0.997
Relative standard deviation ^a (%)	4	3	2.5	3.4
Enrichment factor	6	8	14	13
Concentration range of calibration curve ($\mu\text{g L}^{-1}$)	10-50	0.15-1.2	5-20	2-15

a: $n = 5$ ($50 \mu\text{g L}^{-1} \text{As}^{3+}$; $1 \mu\text{g L}^{-1} \text{Cd}^{2+}$; $20 \mu\text{g L}^{-1} \text{Pb}^{2+}$; $8 \mu\text{g L}^{-1} \text{Se}^{4+}$)

The limits of detection and quantification were calculated according to IUPAC recommendations by means of Equations 4 and 5.³⁶

$$\text{Limit of detection (LOD)} = \frac{3s}{m} \quad \text{Equation 4}$$

$$\text{Limit of quantification (LOQ)} = \frac{10s}{m} \quad \text{Equation 5}$$

in which s is the standard deviation of ten consecutive measurements of the analytical blank and m is the slope of the calibration curve.

The LOD and LOQ values in $\mu\text{g L}^{-1}$ and $\mu\text{g g}^{-1}$ in Table I correspond to instrumental limits (in $\mu\text{g L}^{-1}$) LODs and LOQs, method limits (in $\mu\text{g L}^{-1}$) considering the Inconel 625 sample mass (2.5 g), the digestate diluted to 30 mL, dilution of 200 times for CPE, and respective enrichment factor. Low limits of detection and quantification were achieved, particularly for Cd, demonstrating appropriate sensitivity concerning As, Cd, Pb, and Se determination in Ni alloy.

The maximum specification limits for the analytes in nickel alloys are $50 \mu\text{g L}^{-1}$ (As and 495 Cd), $2 \mu\text{g L}^{-1}$ (Pb), and $1 \mu\text{g L}^{-1}$ (Se) according to AMS 2280. Thus, the LOQs obtained (Table I) comply with the legislation. The obtained linear correlation coefficients values were higher than 0.995, which is highly acceptable for the CPE method. The relative standard deviation, which express the method precision, was below 5% which is acceptable.

The enrichment factor values were considered satisfactory. They were obtained from the ratio of the slopes of the calibration curves constructed with calibration solutions submitted or not to CPE for the respective analytes. When CPE was not used the calibration solutions were matched to the final surfactant-rich phase (matrix-matched calibration curve); containing Triton X-114, and methanol mixed with 0.1 mol L⁻¹ HNO₃.

Sample analysis

The As, Cd, Pb, and Se concentrations found in the Inconel 625 nickel alloy sample and standard reference materials analyzed by following the developed method are given in Table III.

Table III. Arsenic, Cd, Pb, and Se determination in the nickel alloy sample (Inconel 625) and standard reference materials (CRMs) (n = 3)

Analyte		Sample				
		Inconel 625	SRM® 361 (AISI 4340 Steel)	SRM® 362 (AISI 94B17 Steel)	SRM® 363 (Chromium- Vanadium Steel)	SRM® 864 (Nickel alloy UNS N06600)
As	Certified (µg g ⁻¹)	-	170 ± 10	920 ± 5	100 ± 10	-
	Found (µg g ⁻¹)	< LD	173 ± 9	904 ± 11	94 ± 5	< LD
	Added (µg L ⁻¹)	20	-	-	-	20
	Obtained (µg L ⁻¹)	18.6 ± (0.5)	-	-	-	19.9 ± (0.3)
Cd	Certified (µg g ⁻¹)	-	-	-	-	-
	Found (µg g ⁻¹)	< LD	< LD	< LD	< LD	< LD
	Added (µg L ⁻¹)	0.45	0.45	0.45	0.45	0.45
	Obtained (µg L ⁻¹)	0.45 ± (0.01)	0.46 ± (0.01)	0.42 ± (0.03)	0.47 ± (0.01)	0.44 ± (0.02)
Pb	Certified (µg g ⁻¹)	-	-	-	-	-
	Found (µg g ⁻¹)	< LD	< LD	< LD	< LD	< LD
	Added (µg L ⁻¹)	10	10	10	10	10
	Obtained (µg L ⁻¹)	9.1 ± (0.6)	9.5 ± (0.3)	9.4 ± (0.3)	9.8 ± (0.4)	9.7 ± (0.3)
Se	Certified (µg g ⁻¹)	-	-	-	-	-
	Found (µg g ⁻¹)	< LD	< LD	< LD	< LD	< LD
	Added (µg L ⁻¹)	8	8	8	8	8
	Obtained (µg L ⁻¹)	8.1 ± (0.6)	8.2 ± (0.3)	7.6 ± (0.07)	7.0 ± (0.2)	7.7 ± (0.3)

Considering that Inconel 625 contains Ni (65.5%) and Fe (1.1%) capable of forming complexes with DDTP, the interference of these elements on As, Cd, Pb, and Se extraction was investigated. According to Pearson's theory, DDTP is a soft base and tends to interact preferentially with soft acids or intermediated acids such as Cd²⁺, Ni²⁺, or Ag⁺; and besides this, Ni also interferes in CPE due to the high ionic strength.¹⁷ Citric acid helped to eliminate the interference of Ni because it has a masking effect on this element.³⁷ Ascorbic acid aided the elimination of Fe because Fe³⁺ reacts with DDTP, consuming the complexing agent and forming a black precipitate. Upon reaction with ascorbic acid, Fe³⁺ was reduced to Fe²⁺, which does

not form a complex with DDTP.²⁹ Moreover, because both reagents have an acid character, experiments were conducted with and without pH adjustment with HCl.

Arsenic, Cd, Pb, and Se were not detected in the analytical samples, with the exception of As in three CRMs. For this reason, analyte spiking was carried out to assess the method's accuracy. Better analyte recovery was obtained by adding ascorbic acid and HCl to the sample solutions whereas non reproducible results were obtained using citric acid only. The analytes recovery in Inconel samples ranged from 91 to 101% when acid ascorbic and citric acid were used.

For the CRMs SRM[®] 361, SRM[®] 362, and SRM[®] 363, an unpaired t-test of As results showed that they agreed with certified values, and no differences were found for a 95% confidence level and recovery ranged from 88 to 104%.

CONCLUSIONS

This study demonstrated the efficiency of CPE for matrix separation/analyte extraction of As, Cd, Pb, and Se in nickel alloy samples. Among the variables investigated for CPE optimization, DDTP, HCl, and Triton X-114 concentrations were the most meaningful.

The SEM-EDS characterization of the samples identified Fe, Ni and Cr as the major elements and due to the possible interference of Fe³⁺ in CPE, ascorbic acid was added to reduce Fe³⁺ species to Fe²⁺ which does not complex with DDTP. Due to the low concentration of As, Cd, Pb, and Se in Inconel samples (lower than limit of detection), their determination was not possible.

Therefore, the Inconel samples and standard reference materials were spiked with known concentrations of analytes to assess their recovery which presented satisfactory results (88 – 104%) demonstrating that the method is adequate for As, Cd, Pb, and Se determination.

Conflicts of interest

There are no conflicts to declare.

Acknowledgements

The authors are grateful to the “Fundação de Amparo à Pesquisa do Estado de São Paulo” (FAPESP - grant#2012/13230-1) and the “Conselho Nacional de Desenvolvimento Científico e Tecnológico” (CNPq) for financial support. A special acknowledgment is made to the company Equipalcool Sistemas Ltda. for kindly providing the Inconel 625 nickel alloy samples.

REFERENCES

- (1) Shao, X.; Liu, Y.; Li, F.; Wu, J. Progress in analytical methods of composition in nickel-base alloy pipes, ICPTT 2011: Sustainable solutions for water, sewer, gas, and oil pipelines - Proceedings of the International Conference on Pipelines and Trenchless Technology **2011**. [https://doi.org/10.1061/41202\(423\)113](https://doi.org/10.1061/41202(423)113)
- (2) Ashino, T.; Takada, K. Determination of trace amounts of selenium and tellurium in nickel-based heat-resisting superalloys, steels and several metals by electrothermal atomic absorption spectrometry after reductive coprecipitation with palladium using ascorbic acid. *Anal. Chim. Acta.* **1995**, *312*, 157-163. [https://doi.org/10.1016/0003-2670\(95\)00215-L](https://doi.org/10.1016/0003-2670(95)00215-L)
- (3) Wiltsche, H.; Prattes, K.; Knapp, G. A novel approach for an automated liquid/liquid extraction system - principle and application for the determination of several trace contaminants in highly alloyed steels and base alloys. *Anal. Bioanal. Chem.* **2011**, *400*, 2329-2338. <https://doi.org/10.1007/s00216-011-4666-3>
- (4) Shekhar, R.; Arunachalam, J.; Das, N.; Murthy, A. M. S. Determination of Cu, Zn, As, Cd, In, Sn, Pb, and Bi in nickel-based superalloys after multi-matrix separation. *At. Spectrosc.* **2005**, *26*, 191-196. <https://doi.org/10.46770/AS.2005.05.005>

- (5) Weipeng, L.; Zhishan, M.; Sixiao, Q.; Lei, G.; Jianying, H.; Liqiu, G.; Lijie, Q. CS-AFM study on Pb-induced degradation of passive film on nickel-based alloy in high temperature and high pressure water. *Corros. Sci.* **2018**, *144*, 249-257. <https://doi.org/10.1016/j.corsci.2018.08.054>
- (6) SAE Aerospace Material Specification AMS-2280D. *Trace Element Control - Nickel Alloy Castings*, **1992**. Available at: <https://www.sae.org/standards/content/ams2280d/> (Accessed: 07/2023).
- (7) Wiltsche, H.; Günther, D. Capabilities of femtosecond laser ablation ICP-MS for the major, minor, and trace element analysis of high alloyed steels and super alloys. *Anal. Bioanal. Chem.* **2011**, *399*, 2167-2174. <https://doi.org/10.1007/s00216-010-4605-8>
- (8) Sahin, Ç. A.; Efeçinar, M.; Satiroglu, N. Combination of cloud point extraction and flame atomic absorption spectrometry for preconcentration and determination of nickel and manganese ions in water and food samples. *J. Hazard. Mater.* **2010**, *176*, 672-677. <https://doi.org/10.1016/j.jhazmat.2009.11.084>
- (9) Bader, N. R.; Edbey, K.; Telgheder, U. Cloud point extraction as a sample preparation technique for trace element analysis: an overview. *J. Chem. Pharm. Res.* **2014**, *6*, 496-501.
- (10) Ojeda, C. B.; Rojas, F. S. Separation and preconcentration by cloud point extraction procedures for determination of ions: recent trends and applications. *Microchim. Acta.* **2012**, *177*, 1-21. <https://doi.org/10.1007/s00604-011-0717-x>
- (11) Di Giacomo, M.; Bertoni, F. A.; Rocha, M. V.; Nerli, B. B.; Rodríguez, F. Cloud point extraction based on non-ionic surfactants: An ecofriendly tool for recovering papain from papaya latex. *J. Environ. Chem. Eng.* **2022**, *10*, 108762. <https://doi.org/10.1016/j.jece.2022.108762>
- (12) Temel, N. K.; Çöpür, M. Determination of Trace Cobalt (II) in Spices Samples by Ultrasonic Assisted Cloud Point Extraction with Spectrophotometry. *J. Mol. Struct.* **2023**, *1284*, 135433. <https://doi.org/10.1016/j.molstruc.2023.135433>
- (13) Llaver, M.; Wuilloud, R. G. Studying the effect of an ionic liquid on cloud point extraction technique for highly efficient preconcentration and speciation analysis of tellurium in water, soil and sediment samples. *Talanta* **2020**, *212*, 120802. <https://doi.org/10.1016/j.talanta.2020.120802>
- (14) Silva, S. G.; Oliveira, P. V.; Rocha, F. R. P. A green analytical procedure for determination of copper and iron in plant materials after cloud point extraction. *J. Braz. Chem. Soc.* **2010**, *21*, 234-239. <https://doi.org/10.1590/S0103-50532010000200007>
- (15) Sorouraddin, S. M.; Farajzadeh, A. M.; Okhravi, T. A green solventless temperature-assisted homogeneous liquid-liquid microextraction method based on 8-hydroxyquinoline simultaneously as complexing agent and extractant for preconcentration of cobalt and nickel from water and fruit juice samples. *Int. J. Environ. Anal. Chem.* **2019**, *99*, 124-138. <https://doi.org/10.1080/03067319.2019.1578351>
- (16) Pytlakowska, K.; Kozik, V.; Dabioch, M. Complex-forming organic ligands in cloud-point extraction of metal ions: A review. *Talanta* **2013**, *110*, 202-228. <https://doi.org/10.1016/j.talanta.2013.02.037>
- (17) Ramos, J. C.; Curtius, A. J.; Borges, D. L. G. Diethyldithiophosphate (DDTP): A review on properties, general applications, and use in analytical spectrometry. *Appl. Spectrosc. Rev.* **2012**, *47*, 583-619. <https://doi.org/10.1080/05704928.2012.682286>
- (18) Castor, J. M. R.; Portugal, L.; Ferrer, L.; Hinojosa-Reyes, L.; Guzmán-Mar J. L.; Hernández-Ramírez, A.; Cerdà, V. An evaluation of the bioaccessibility of arsenic in corn and rice samples based on cloud point extraction and hydride generation coupled to atomic fluorescence spectrometry. *Food Chem.* **2016**, *204*, 475-482. <https://doi.org/10.1016/j.foodchem.2016.02.149>
- (19) Maranhão, T. A.; Martendal, E.; Borges, D. L. G.; Carasek, E.; Welz, B.; Curtius, A. J. Cloud point extraction for the determination of lead and cadmium in urine by graphite furnace atomic absorption spectrometry with multivariate optimization using Box-Behnken design. *Spectrochim. Acta, Part B* **2007**, *62*, 1019-1027. <https://doi.org/10.1016/j.sab.2007.05.008>

- (20) Borges, D. L. G.; Veiga, M. A. M. S.; Frescura, V. L. A.; Welz, B.; Curtius, A. J. Cloud-point extraction for the determination of Cd, Pb and Pd in blood by electrothermal atomic absorption spectrometry, using Ir or Ru as permanent modifiers. *J. Anal. At. Spectrom.* **2003**, *18*, 501-507. <https://doi.org/10.1039/B209680C>
- (21) Depoi, F. S.; Oliveira, T. C.; Moraes, D. P.; Pozebon, D. Preconcentration and determination of As, Cd, Pb and Bi using different sample introduction systems, cloud point extraction and inductively coupled plasma optical emission spectrometry. *Anal. Methods* **2012**, *4*, 89-95. <https://doi.org/10.1039/C1AY05246B>
- (22) Kassem, M. A.; Amin, A. S. Determination of rhodium in metallic alloy and water samples using cloud point extraction coupled with spectrophotometric technique. *Spectrochim. Acta Part A* **2015**, *136*, 1955-1961. <https://doi.org/10.1016/j.saa.2014.10.116>
- (23) Stefanova-Bahchevanska, T.; Milcheva, N.; Zaruba, S.; Andruch, V.; Delchev, V.; Simitchiev, K.; Gavazov, K. A green cloud-point extraction-chromogenic system for vanadium determination. *J. Mol. Liq.* **2017**, *248*, 135-142. <https://doi.org/10.1016/j.molliq.2017.10.046>
- (24) Bakkar, A.; Ahmed, M. M. Z.; Alsaleh, N. A.; Seleman, M. M. E.; Ataya, S. Microstructure, wear, and corrosion characterization of high TiC content Inconel 625 matrix composites. *Mater. Res. Technol.* **2019**, *8*, 1102-1110. <https://doi.org/10.1016/j.jmrt.2018.09.001>
- (25) Borowski, T.; Brojanowska, A.; Kost, M.; Garbacz, H.; Wierzchoń, T. Modifying the properties of the Inconel 625 nickel alloy by glow discharge assisted nitriding, *Vacuum* **2009**, *83*, 1489-1493. <https://doi.org/10.1016/j.vacuum.2009.06.056>
- (26) Stalikas, C. D. Micelle-mediated extraction as a tool for separation and preconcentration in metal analysis. *Trends Anal. Chem.* **2002**, *21*, 343-355. [https://doi.org/10.1016/S0165-9936\(02\)00502-2](https://doi.org/10.1016/S0165-9936(02)00502-2)
- (27) Fiorentini, E. F.; Canizo, B. V.; Wuilloud, R. G. Determination of As in honey samples by magnetic ionic liquid-based dispersive liquid-liquid microextraction and electrothermal atomic absorption spectrometry. *Talanta* **2019**, *198*, 146-153. <https://doi.org/10.1016/j.talanta.2019.01.091>
- (28) Mortada, W. I. Recent developments and applications of cloud point extraction: A critical review. *Microchem. J.* **2020**, *157*, 105055 <https://doi.org/10.1016/j.microc.2020.105055>
- (29) Silva, M. A. M.; Frescura, V. L. A.; Aguilera, F. J. N.; Curtius, A. J. Determination of Ag and Au in geological samples by flame atomic absorption spectrometry after cloud point extraction. *J. Anal. At. Spectrom.* **1998**, *13*, 1369-1373. <https://doi.org/10.1039/A806309E>
- (30) Mandal, S.; Lahiri, S. A review on extraction, preconcentration and speciation of metal ions by sustainable cloud point extraction. *Microchem. J.* **2022**, *175*, 107150. <https://doi.org/10.1016/j.microc.2021.107150>
- (31) Anzum, R.; Alawamleh, H. S. K.; Bokov, D. O.; Jalil, A. T.; Hoi, H. T.; Abdelbasset W. K.; Thoi, N. T.; Widjaja, G.; Kurochkina, A. A review on separation and detection of copper, cadmium, and chromium in food based on cloud point extraction technology. *Food Sci. Technol.* **2022**, *42*, 1-7. <https://doi.org/10.1590/fst.80721>
- (32) Rihana-Abdallah, A.; Li, Z.; Lanigan, K. C. Using Cloud Point Extraction for Preconcentration and Determination of Iron, Lead, and Cadmium in Drinking Water by Flame Atomic Absorption Spectrometry. *Anal. Lett.* **2022**, *55*, 1296-1305. <https://doi.org/10.1080/00032719.2021.2002349>
- (33) Silva, M. A. M.; Frescura, V. L. A.; Curtius, A. J. Determination of trace elements in water samples by ultrasonic nebulization inductively coupled plasma mass spectrometry after cloud point extraction. *Spectrochim. Acta B* **2000**, *55*, 803-813.
- (34) Smrkolj, P.; Stibilj, V. Determination of selenium in vegetables by hydride generation atomic fluorescence spectrometry. *Anal. Chim. Acta* **2004**, *512*, 11-17. <https://doi.org/10.1016/j.aca.2004.02.033>
- (35) Kretzschmar, J.; Jordan, N.; Brendler, E.; Tsushima, S.; Franzen, C.; Foerstendorf, H.; Stockmann, M.; Heim, K.; Brendler, V. Spectroscopic evidence for selenium(IV) dimerization in aqueous solution, *Dalton Trans.* **2015**, *44*, 10508-10515. <https://doi.org/10.1039/C5DT00730E>

- (36) Harris, D. C. *Quantitative Chemical Analysis*, 7th Edition, 2007, W. H. Freeman and Company New York.
 (37) Danadurai, K. S. K.; Hsu, Y.; Jiang, S. Determination of selenium in nickel-based alloys by flow injection hydride generation reaction cell inductively coupled plasma mass spectrometry. *J. Anal. At. Spectrom.* **2002**, *17*, 552-555. <https://doi.org/10.1039/B202878F>

Supplementary Material

Table SI. Instrumental parameters for As, Cd, and Se determination after cloud point extraction using AAnalyst 800 (PerkinElmer)

Parameter	Condition
Wavelength (nm)	193.7 ^a , 228.8 ^b , 196.0 ^c
Radiation source	Hollow cathode lamps of As, Cd, and Se
Electrical current (mA)	18 ^a , 8 ^b , 25 ^c
Slit (nm)	0.7 ^{a,b} , 2 ^c
Argon flow (mL min ⁻¹)	250
Background correction	Longitudinal Zeeman Effect

a = As; b = Cd; c = Se.

Table SII. Instrumental parameters for Pb determination after cloud point extraction using ContrAA 700 (Analytik Jena)

Parameter	Condition
Wavelength (nm)	283.3060
Radiation source	Short-arc lamp of Xenon
Electrical current (A)	13
Argon flow (L min ⁻¹)	2
Background correction	Simultaneous background correction

Table SIII. Graphite furnace temperature program for As, Cd, and Se determination after cloud point extraction using AAnalyst 800 (PerkinElmer)

Step	Temperature (°C)	Ramp (s)	Hold (s)	Ar flow rate (mL min ⁻¹)
Drying	110	1	30	250
Drying	130	15	30	250
Pyrolysis	(800 ^a , 1200 ^b) ¹ ; (600 ^a , 500 ^b) ² ; (900 ^{a,b}) ³	10	20	250
Atomization	(2000 ^{a,b}) ¹ ; (1700 ^a , 1300 ^b) ² ; (1900 ^a , 1800 ^b) ³	0	5	0
Cleaning	2450	1	3	250

1 = As; 2 = Cd; 3 = Se; a = optimization of the CPE experimental parameters; b = after obtainment of the pyrolysis and atomization curves.

Table SIV. Graphite furnace temperature program for Pb determination after cloud point extraction using ContrAA 700 (Analytik Jena)

Step	Temperature (°C)	Ramp (°C s ⁻¹)	Hold (s)	Air flow rate (L min ⁻¹)
Drying	90	3	20	2
Drying	110	5	10	2
Pyrolysis	900 ^a , 1000 ^b	300	10	2
Atomization	1900 ^{a,b}	3000	3	0
Cleaning	2450	500	4	2

a = optimization of the CPE experimental parameters; b = after obtainment of the pyrolysis and atomization curves.